

# **PRESSUREMETER TESTS IN POORLY CEMENTED WEAK ROCKS**

by

A. B. Huang, I. W. Pan, J. J. Liao,  
C. H. Wang and S. Y. Hsieh

*Reprinted from  
Proceedings of the 37th U.S. Rock Mechanics,  
June, 1999, Vail, Colorado, pp.247-252*

# Pressuremeter tests in poorly cemented weak rocks

A. B. Huang, I. W. Pan & J. J. Liao

*Department of Civil Engineering, National Chiao Tung University, Hsin Chu, Taiwan*

C. H. Wang

*Geotechnical Engineering Department 1, Moh and Associates Incorporated, Taipei, Taiwan*

S. Y. Hsieh

*Institute of Planning and Hydraulic Research, Taiwan Provincial Water Conservancy, Tai Chung, Taiwan*

**ABSTRACT:** A series of pre-bored pressuremeter tests (PMT) were performed in relatively young, weak rock deposits at several test sites in Taiwan. Equipment used included the Ménard type tri-cell pressuremeter and Cambridge high-pressure dilatometer. The test data were interpreted using some of the existing empirical and a newly developed analytical procedure. According to the interpretations of PMT data, the tested weak rock should behave as a highly overconsolidated cohesive material. This is contrary to some of the available laboratory experimental results. A 3-surface numerical scheme has been developed to simulate pressuremeter expansion in weak rock with unload-reload cycles. Preliminary results have indicated that the numerical scheme is capable of capturing the important features of pressuremeter expansion in a weak sandstone.

## 1 INTRODUCTION

The outcrops in the northern and central regions of Western Taiwan often contain very weak, young and weakly cemented rocks. These sedimentary rocks were formed in epochs from late Miocene to Pleistocene. Unconfined compressive strengths of these rocks are typically less than 25 MPa, which characterizes them as weak rocks. The conventional sampling process with core barrels is likely to damage the structure that originally existed in the rock formation. The uniaxial strengths obtained in laboratory experiments are often scattered. Pressuremeter test (PMT) is an in situ testing method that has the potential of avoiding some of the problems inherent to laboratory testing. The authors analyzed a series of PMT at five test sites to evaluate the characteristics of PMT in these weak rock deposits. Pressuremeter equipment used included the Ménard type tri-cell pressuremeter and Cambridge High Pressure Dilatometer. Field shear wave velocity measurements, coring of rock samples and laboratory experiments were performed at selected test sites to provide reference parameters. This paper analyzes the available PMT data from empirical as well as analytical point of view and discusses the characteristics of these PMT in the weak rock.

## 2. THE TEST SITES AND PMT TEST PROCEDURE

The test sites are scattered in central and northern Taiwan as shown in Figure 1. Test Site 1 is located in a residential development project area in Tai-Chung County. The predominant rock formation contains interbeds of sandstone and shale from Pliocene-Pleistocene. The unconfined compressive strength ( $q_u$ ) from tests on rock cores taken at Test Site 1 ranged from 1.6 – 29.6 MPa. Triaxial tests indicated cohesion values,  $c$  of 0.27 – 3.6 MPa and friction angle ( $\phi$ ) in a range of 45 – 50 degrees. Test Site 2 is situated at the northern entrance of a proposed High Speed Rail tunnel, in Miao-Li County. The majority of PMT were performed in layers of Pleistocene sandstone and mudstone. Test Site 3 sits in a Buddhist temple development complex in Tai-Chung County. The soil/rock formation at Test Site 3 is of colluvial/sedimentary in nature. The parental rock similar to those at Test Site 1 collapsed and resettled at its current position less than 10,000 years ago. Test Site 4 is located at a proposed earth dam project area in Hsin-Chu County. PMT were performed in Pleistocene sandstone, shale and mudstone formations. The  $q_u$  from tests on rock cores taken at Test Site 4 ranged from 0.2 – 1.2 MPa. Triaxial tests indicated  $c$  of 0.2 – 1.2 MPa and  $\phi$  in a range of 25 – 45 degrees. Test Site 5 is situated within a high-rise building development project area in Taipei City. The PMT

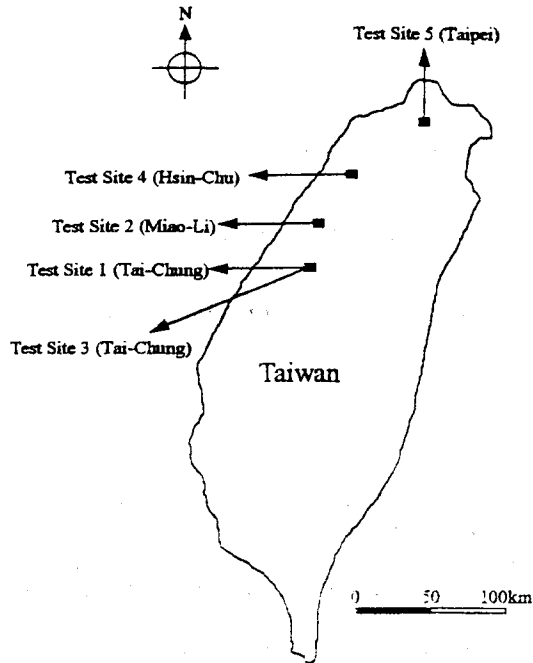


Figure 1. Test site locations.

were conducted in a late Miocene sandstone formation. Table 1 shows a summary of the PMT to be described in the paper and the rock formations where the PMT was performed. The authors performed all the PMT at Test Sites 1 through 4, one borehole per test site, using a Ménard type tri-cell pressuremeter. The PMT at Test Site 5 were conducted by a consulting engineering firm using a Cambridge high-pressure dilatometer. The PMT at Test Site 5 were distributed in four boreholes. Downhole seismic shear wave velocity measurements were also taken in the vicinity of the boreholes to provide reference initial shear modulus ( $G_0$ ) values.

The water inflated Ménard type tri-cell pressuremeter has an initial probe diameter of 73mm. The measurement cell has a length to diameter ratio (L/D) of 4. The maximum pressure applicable to

the Ménard pressuremeter is 6 MPa. No unload-reload loops were applied in the PMT using Ménard pressuremeter. The Cambridge High Pressure Dilatometer (HDP) has a diameter of 73mm and an expanding length of 450mm (L/D = 6.2). HPD can be inflated by compressed nitrogen or hydraulic fluid to a maximum pressure of 20MPa. The HPD probe is equipped with six radially positioned strain arms equally spaced around the center of the probe. The PMT using HPD had one to two unload-reload loops during the expansion stage and some of the tests had one unload-reload loops in the unloading phase of the test. A waiting period of 5 minutes was given prior to the unload-reload cycle to minimize material creeping. The majority of unload-reload loops had a maximum strain difference ( $\Delta\varepsilon$ ) of 0.4%. The pressure reduction or "loop depth" ( $\Delta p$ ) did not exceed 40% of the expansion pressure at the beginning of the loop ( $p_i$ ). The  $\Delta p/p_i$  ratio is conservatively lower than the criterion proposed by Fahey (1991), considering the potential strength of the weak rock. All PMT followed a stress controlled test procedure. For each stress increment, the probe pressure was held constant for a period of 60 seconds. The difference in probe expansion between 30 and 60 second after the stress increment is referred to as the creep volume (PMT) or creep strain (HPD). Figure 2 shows a typical PMT expansion curve using the Ménard probe and Figure 3 displays an expansion curve from a tests using the HPD.

### 3. EMPIRICAL EVALUATION OF PMT IN WEAK ROCK

The available data were analyzed empirically first to evaluate the feasibility of using some of the concepts developed for PMT in soils and to establish index parameters for PMT in weak rocks. For the results from Test Sites 1 through 4, the initial lift-off pressure ( $P_0$ ), yield pressure ( $P_y$ ), limit pressure ( $P$ )

Table 1. Summary of the PMT.

Test Site No.	Types of rock formations	Epoch of rock formation	Estimated age of rock formation	Number of PMT performed	Range of Depth, m
1	Shale	Pliocene-Pleistocene	2 - 3 million years	3	9 - 15
2	Sandstone, mudstone	Pleistocene	1 - 2 million years	8	5 - 24
3	Sandstone, shale	N/A	< 10,000 years	9	7 - 28
4	Sandstone, shale, mudstone	Pleistocene	4 - 5 million years	6	12 - 28
5	Sandstone	Miocene	8 million years	26	45 - 98

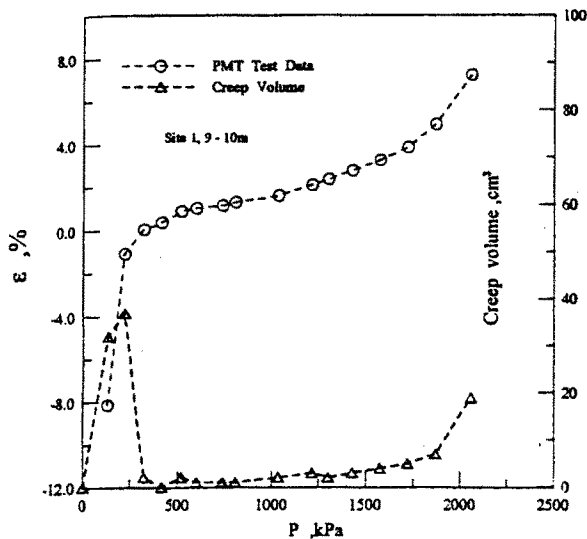


Figure 2. Typical PMT expansion curve using the Ménard probe.

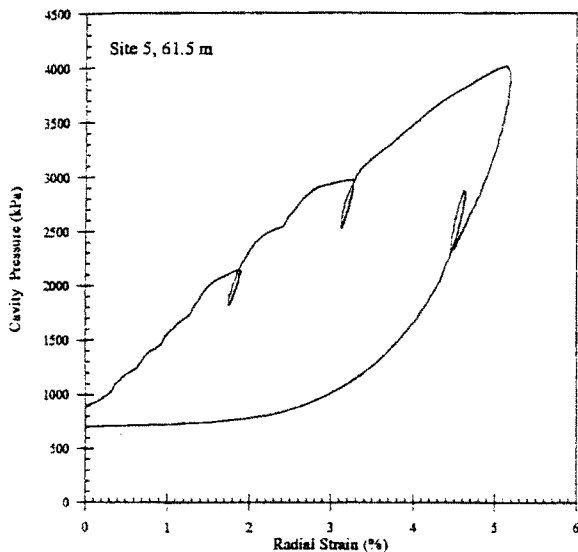


Figure 3. PMT expansion curve from a test using HPD.

and pressuremeter modulus ( $E_m$ ).  $P_0$  corresponds to the pressure where the creep volume drops to a minimum in the initial stage of the pressuremeter expansion. The creep volume remains steady as the expansion continues until  $P_y$  is reached where creep volume starts increasing.  $P_1$  is defined as the pressure where the probe volume reaches twice the original cavity volume. The pressuremeter modulus is calculated as:

$$E_m = 2(1-\nu) \left( V_0 + \frac{V_y + V_1}{2} \right) \frac{P_y - P_0}{V_1 - V_0} \quad (1)$$

where

$V_0$  = probe volume that corresponds to  $P_0$ ;  
 $V_y$  = probe volume that corresponds to  $P_y$ ;  
 $\nu$  = Poisson's ratio assumed to be 0.3.

Figure 4 shows a plot of  $P_0$ ,  $P_y$ , and  $P_1$  versus depth. It is generally believed that  $P_0$  can be an indication of the in situ lateral stress. For the measurements shown in Figure 4, except for the results at Test Site 2, the  $P_0$  values are too low to have any meaningful indication of in situ lateral stress. It is likely that the borehole drilling had severely disturbed the surrounding material to reflect the in situ lateral stress. The  $P_y$  and  $P_1$  are related to the strength parameters of the surrounding material (Haberfield and Johnston, 1990). Results of  $P_y$  and  $P_1$  indicate a slightly positive but consistent relationship with depth. The consistency of test data is a reflection of young rock formations with limited discontinuities at the test site. Table 2 shows the available  $E_m/P_1$  values and arranged in accordance with the geological age of the rock formations. These  $E_m/P_1$  values are well within the range of weathered rock as reported by Clarke (1995). There appears to be a strong and positive relationship between  $E_m/P_1$  and age of the rock formation. The  $P_1$  and  $E_m/P_1$  values correspond to results typically found in cohesive materials. This is somewhat contradictory to the available laboratory experiments on rock cores that showed substantial friction angles and relatively low cohesion values.

The PMT at Test Site 5 using HPD had a high initial pressure increment that essentially eliminated the possibility of estimating  $P_0$ . Because of the relatively high strength of the rock, most of the PMT were terminated right after  $P_y$  was reached or in some cases before  $P_y$ . Significant judgement is

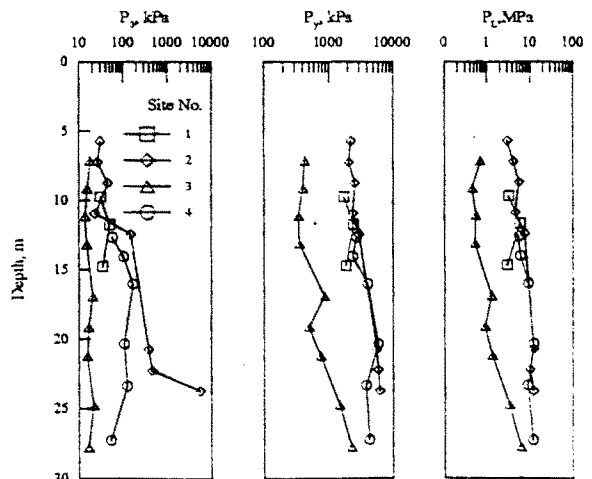


Figure 4.  $P_0$ ,  $P_y$ , and  $P_1$  versus depth.

Table 2.  $E_m/P_i$  from the PMT at Test Sites 1 to 4.

	Age of the rock formation, years			
	< 10,000	1 - 2 million	2 - 3 million	4 - 5 million
	Test Site No.			
Rock type	3	2	1	4
Sandstone	7 - 18	15 - 23		23 - 38
Shale	10		17 - 32	49
Mudstone		18 - 21		28

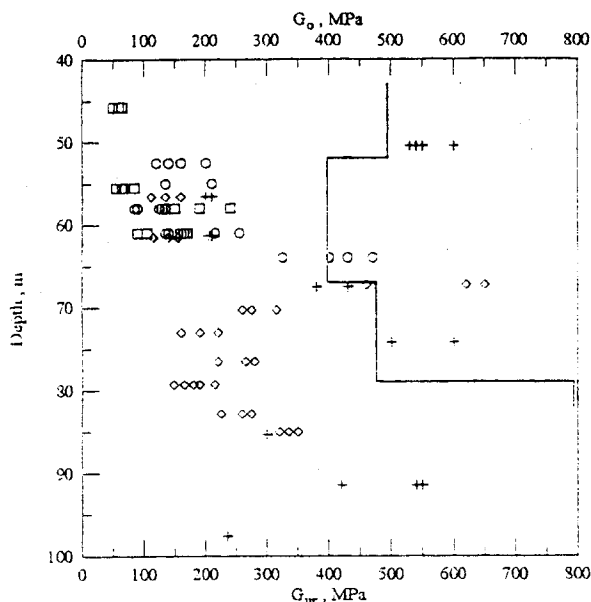


Figure 5.  $G_{ur}$  and  $G_0$  versus depth.

required in extrapolating for the  $P_i$  value from the test data. Because of these reasons, the data from Test Site 5 were not analyzed in terms of the parameters shown in Table 2. The tests with HPD had unload-reload loops, however, that allows the unload-reload shear modulus ( $G_{ur}$ ) be evaluated against  $G_0$  from the downhole shear wave velocity measurements.  $G_{ur}$  is assessed by drawing a best-fit line through the unload-reload loop ( $G_{ur} = 0.5(\Delta p / \Delta \epsilon)$ ). Figure 5 shows a plot of  $G_{ur}$  from tests with the HPD and  $G_0$  versus depth. According to Figure 5, the majority of  $G_{ur}/G_0$  falls in a range of 0.3 to 0.6. These values are relatively low compared to those reported for sands (Fahey, 1998). A few data points showing  $G_{ur}/G_0$  in excess of 1 are likely to be a localized abnormality not detected by the downhole seismic test.

#### ANALYTICAL EVALUATION OF PMT IN WEAK ROCK

When analyzing the PMT data in a rigorous manner, the interpretation method should be able to capture

some of the important mechanical characteristics of weak rocks. Upon unloading (e.g., due to sampling), a weak rock specimen usually exhibits a strain hardening behavior during the early stage of an axial compression test. The strain hardening is associated with the crack closure caused by the axial compression. Similar phenomenon is expected to occur for pre-bored PMT in weak rock during the early stage of pressuremeter expansion (i.e., compression) as bore hole preparation causes unloading to the surrounding rock mass. As PMT continues to expand, crack is likely to occur again due to the decrease in circumferential stress. The use of HPD involves unload-reload loops. The capability of keeping track of stress history becomes a highly desirable feature in analyzing this type of PMT. Haberfield and Johnston (1990) proposed a rigorous interpretation method for PMT in weak rock under monotonic loading conditions. Numerical schemes to describe the unload-reload loops of PMT in soils have also been reported (Byrne et al., 1990; and Fahey, 1998). These available methods lack the ability to combine all aspects that are required for a proper description of weak rock during PMT. The authors developed a numerical model that is capable of considering the crack closure/opening as well as unload-reload behavior during a PMT in weak rock.

The stress-strain relation of a soft rock is highly dependent of its stress-path and stress-history. Various multi-surface models (Dafalias, 1986; Mroz et al., 1981; Pietruszczak and Poorooshasb, 1987; and Prevost, 1978) have demonstrated their effectiveness and capability in modeling the inelastic behavior of geomaterials under both monotonic and cyclic loads. Among several of the available multi-surface models, the generalized transitional yielding approach (Pan and Banerjee, 1987; and Pan, 1991) with any desired number of limit-surfaces, can represent various degree of hierarchical material memory due to stress-history. The 3-surface model, a special version of the generalized transitional yielding approach, is adopted for modeling the mechanical behavior of weak rock in the presented work. The following presents a brief outline of the transitional yielding approach.

#### 4.1 The Transitional Yielding Approach

The fundamental assumption of the transitional yielding model (Pan and Banerjee, 1987) is the existence of a bounding surface and a loading surface. The bounding surface is expressed as

$$f(\sigma, a_b) = 0 \quad (2)$$

in which " $a_b$ " is the size of the bounding surface (" $a_b$ " can be regarded as a hardening parameter). Similar to the bounding surface, a loading surface is expressed as a function of a transformed stress-state  $\sigma^*$  and a yielding ratio  $s$ . The loading surface satisfies

$$f(\sigma^*, a) = 0 \quad (3)$$

In the above function: " $a$ " is the size of current loading surface and  $\sigma^*$  is the transformed stress state defined as  $\sigma^* = \sigma - (1-s)\sigma^R$ , in which  $\sigma^R$  is the stress tensor at the instance of the most recent stress reversal and " $s$ " is yielding ratio. The yielding ratio  $s$  is defined as the ratio of the size of the loading surface to the size of the bounding surface, i.e.,  $s = a/a_b$ ,  $0 < s < 1$ . A stress-reversal condition occurs whenever  $s$  suddenly decreases. When a stress-reversal occurs, the stress-state at the instance of stress-reversal becomes the new  $\sigma^R$ , and the loading surface collapses to a point. Concurrently, the yielding ratio  $s$  drops to zero. Subsequently, the loading surface starts to evolve (expand and translate) along with the change in stress-state.

Any change in the stress-state,  $\delta\sigma$  may result in a variation of the function of loading surface,  $\delta f$ . A change in the yielding ratio,  $\delta s$ , has to accompany with  $\delta\sigma$  in order to maintain  $f = 0$ . The yielding ratio  $s$  can be updated using an incremental approach by iteration.

The concept of the transitional yielding approach is further extended to include any desired number of nesting limit surfaces for the representation of a higher degree material memory (Pan, 1991). For a 3-surface model, one limit surface lies between the bounding surface and the current loading surface. This limit surface is the last loading surface before the stress reversal occurs. It represents the material's memory of the last stress segment. In the 3-surface model, the transformed stress-state is defined as follows.

$$\sigma^* = (\sigma - \sigma_1) - (1 - s_2)(\sigma_2^R - \sigma_1) \quad (4)$$

In the above equation,  $\sigma_1 = (1 - s_1)\sigma_1^R$  in which

$s_1 = a_1/a_b$ ,  $s_2 = a/a_1$ , and  $s = a/a_b = s_1 s_2$ ;  $a$ ,  $a_1$ , and  $a_b$ , respectively, are the sizes of the loading surface, the limit surface, and the bounding surface, respectively. The ratio  $s_1$ ,  $s_2$ , and  $s$  are real numbers on the interval  $[0, 1]$ .  $\sigma_2^R$  is the stress-state when the most recent stress-reversal occurs:  $\sigma_1^R$  is

the stress-reversal state corresponding to the limit surface. If the current loading surface is the largest one that the material has experienced, then the current loading surface coincides with the limit surface; hence  $a = a_b$  and  $s_2 = 1$ . In that case,  $\sigma_2^R$  is set equal to  $\sigma_1^R$ . The limit-surface in the 3-surface model represents the hierarchical material memory due to stress history. With the transitional yielding model, the effects of stress-history and stress-path are taken into account naturally.

As the loading surface gradually approach to the bounding surface (the yielding ratio  $s$  gradually approaches to 1.0), the deformability of the material decreases with the increasing yielding ratio  $s$ . To model the gradual degradation of weak sandstone, its material modulus is related to the yielding ratio as follows.

When  $s_2 = 1$  (i.e.,  $a = a_b$ ):

$$E = E_v = (1 - s_1^{\gamma_1})E_v \quad (5)$$

in which  $E_v$  is the modulus during virgin loading ( $a = a_b$ ). The above relation has the property of  $E \rightarrow 0$  as  $s_1 \rightarrow 1.0$ .

When  $s_2 < 1$  (i.e.,  $a < a_b$ ):

$$E = E_v = (1 - s_2^{\gamma_2})E_v \leq E_v \quad (6)$$

The parameters  $\gamma_1$ ,  $\gamma_2$ ,  $E_v$ , and  $E_u$  are material parameters.  $E_v$  is the Young's modulus for virgin loading;  $E_u$  is the Young's modulus for small-strain unloading/reloading. To further model the effect of crack-closure during early loading stage,  $E_v$  is expressed as a function of the octahedral normal stress for  $\sigma_{oct} < p_1$  as follows.

$$E_v = E_A + (E_B - E_A) \left( \frac{\sigma_{oct}}{p_1} \right)^{\gamma_3} \text{ for } \sigma_{oct} < p_1 \quad (7)$$

The multi-surface approach does not require a particular form of the yield surface. This model is applicable for nonlinear numerical analyses of boundary-value problems.

#### 4.2 Numerical Simulation of PMT in Weak Sandstone

Numerical simulation using a non-linear finite-element code incorporating the transitional yielding model was carried out to simulate the PMT shown in Figure 3. The Hoek-Brown yield criterion for intact rock (i.e.,  $\sigma_1 - \sigma_3 = \sqrt{m\sigma_c\sigma_3 + \sigma_c^2}$ ), is adopted as the yield surface of the weak sandstone. The input parameters are as follows:  $m=10$ ,  $\sigma_c=4$ ,  $E_B=200\text{MPa}$ ,  $E_A=100\text{MPa}$ ,  $E_u=6E_v$ ,  $p_1=1.5\text{MPa}$ ,  $\gamma_1=4$ ,  $\gamma_2=0.5$ , and  $\gamma_3=1$ . The selection of these parameters considers the available shear wave velocity measurements in the vicinity and characteristics of a

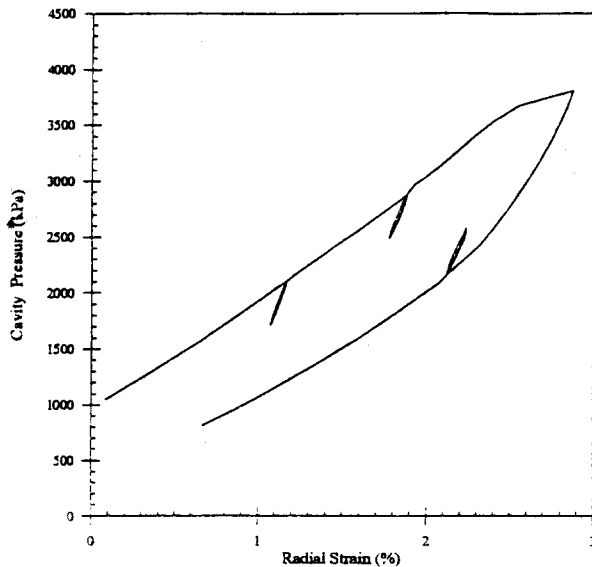


Figure 6. Simulated PMT expansion curve in weak rock.

weak sandstone. The PMT was simulated as an axial symmetrical cavity expansion with the fixed boundary located at 20 times of the initial cavity radius from the axis of symmetry. The initial stress-state of the weak rock before the cavity expansion was assumed uniform and isotropic. The initial cavity-pressure was incrementally changed subsequently. Figure 6 presents the result of the cavity expansion simulation in terms of cavity pressure against the radial strain. In comparison with the results depicted in Figure 3, it seems that the simulation can substantially capture the trend of in-situ experimental results.

## 5. CONCLUSIONS

Because of the difficulties in recovering good quality samples, PMT can be a viable alternative in characterizing the behavior of weak rocks in situ. In the cases presented in the paper, PMT provided data with much improved consistency in comparison with laboratory data. For the PMT conducted in weak sandstone, shale and mudstone, reflect mostly the behavior of a cohesive material. According to the laboratory experiments, the weak rocks are mostly frictional in nature. It is likely that a substantial part of the cohesive nature of the rock cores was destroyed in the process of sampling.

The  $E_m/P_i$  values obtained from PMT, using the Ménard type tri-cell pressuremeter, generally falls in the range of weathered rock and can be expected to increase with the age of the rock formation. According to the PMT in sandstone using a HPD,  $G_{ur}/G_o$  varied from 0.3 to 0.6, which is slightly lower

than those reported for sands. Preliminary results have indicated that a 3-surface model, a special version of the generalized transitional yielding approach, is capable of capturing the important features of pressuremeter expansion in a weak sandstone. It appears feasible that the Hoek-Brown yield parameters as well as the rock deformability can be back calculated by curve fitting the PMT data with this numerical model.

## REFERENCES

- Byrne, P.M., Salgado, F.M., and Howie, J.A., 1990. Relationship between the Unload-Reload Modulus from Pressuremeter Tests and The Maximum Shear Modulus for Sand. Proceedings, 3<sup>rd</sup> International Symposium on Pressuremeters, Oxford, UK, pp.231-241.
- Clarke, B.G., 1995. Pressuremeters in Geotechnical Design. Blackie and Academic and Professional, Glasgow, UK, 364p.
- Dafalias, Y. F., 1986. Bounding Surface Plasticity. I: Mathematical Foundation and Hypoplasticity. *J. Engrg. Mech.*, ASCE, 112(9), 966-987.
- Fahey, M., 1991. Measuring Shear Modulus in Sand with the Self-Boring Pressuremeter. Proceedings, 10th European Conference on SMFE, Florence, Italy, Vol.1, pp.73-76, Balkema, Rotterdam.
- Fahey, M., 1998. Deformation and In Situ Stress Measurement. Proceedings, 1st International Conference on Site Characterization, Atlanta, Georgia, Vol.1, pp.49-68, Balkema, Rotterdam.
- Haberfield, C.M. and Johnston, I.W., 1990. The interpretation of pressuremeter tests in weak rock-theoretical analysis. Proc. 3rd Int. Symp. Pressuremeter, Oxford, pp. 169-178.
- Mroz, Z., Norris, V. A. and Zienkiewicz, O. C., 1981. An Anisotropic, Critical State Model for Soils Subject to Cyclic Loading. *Geotechnique*, 31(4), 451-469.
- Pietruszczak, S. and Porooshasb, H. B., 1987. On Yielding and Flow of Sand: a Generalized Two-surface Model. *Computers and Geomechanics*, 1, pp. 33-58.
- Prevost, J. H., 1978. Anisotropic Undrained Stress-strain Behavior of Clays. *J. Geotech. Engrg.*, ASCE, 104(8), 1075-1090.
- Pan, Y. W. and Banerjee, S., 1987. Transitional Yielding Approach for Soils under General Loading. *J. of Engrg. Mech.*, ASCE, 113(2), 153-169.
- Pan, Y. W., 1991. A generalized Non-associative Multi-surface Approach for Granular Materials. *J. of Geotechnical Engrg.*, ASCE, 117(1).